

Study on the Degradation Mechanism of the Cyclopentaneoxygen free radicals: $c\text{-C}_5\text{H}_9$ Radical with $\text{O}(\text{}^3\text{p})$ radical

Hongxia Liu^{a,b*}

^a.Department of Chemistry, Anshan Normal University, Anshan 114007, China

^b.Chemistry and Environment Science College, Inner Mongolia Key Laboratory of Green Catalysis, Inner Mongolia Normal University, Hohhot 010022, China)

Abstract: The degradation reaction mechanism of $c\text{-C}_5\text{H}_9\text{O}$ has been investigated theoretically by a detailed potential energy surface calculation at the B3LYP/6–311G(d,p) and MC–QCISD (single-point) levels of theory. Starting from the reactant, the most favorable pathway is the $\beta\text{-C-C}$ bond dissociation to form intermediate **b** ($\text{CH}_2\text{)CHO}$. The second competitive pathway are the 1,3-H-shift leading to product **P1** $c\text{-C}_5\text{H}_8\text{OH}$, which can further dissociate to give **P3** $c\text{-C}_5\text{H}_8 + \text{OH}$ and C-H bond cleavage to form **P2** $c\text{-C}_5\text{H}_8\text{O} + \text{H}$. While the formation of the products **P4** - **P9** derived from intermediate **b** are less competitive than products **P1** – **P3**. Our calculations show that the intermediates and transition states involved in the above product channels all lie above the reactants, the $c\text{-C}_5\text{H}_9\text{O}$ degradation reaction is expected to be unrapid, as is confirmed by experiment. So we can try to control the pressure and the temperature to gain our ends. The present results may be helpful for understanding the mechanism and can assist in experiments to identify the products of the title reaction.

Keywords: Theoretical study; PESs; DFT; Reaction mechanism; Rate constants

Date of Submission: 27-05-2019

Date of acceptance: 11-06-2019

I. Introduction

Radical–radical cross-combination reactions constitute an integral part of the overall mechanisms of oxidation hydrocarbons [1,2]. A variety of anthropogenic sources can release the cycloalkanes into the atmosphere [3,4]. The oxidation of them leads to the formation of secondary pollutants (e.g., ozone, aldehydes, ketones, aerosols), and thus contributes to the degradation of air quality in and around urban regions. There are a lot of laboratory investigations and theoretical mechanisms of the cycloalkoxy which have been carried out [5-14]. Alkoxy radicals normally cleave to give a ketone (or aldehyde) and the most stable possible alkyl radical [15].

The kinetic study has been performed on the diradical reaction $c\text{-C}_5\text{H}_9$ with O. This reaction can easily form free radical $\text{C}_5\text{H}_9\text{O}$. Oxygenated radicals, such as phenoxy ($\text{C}_6\text{H}_5\text{-O}\cdot$) play a large role in biological and environmental processes as transient species.1 Substituted or metal-complexed phenoxy radicals are commonly encountered in larger biomolecules such as microperoxidase and galactooxidase2 – important compounds in biocatalysis.3 In addition, phenoxy moieties are common linkages in lignin macromolecules, which can be cracked by fast-pyrolysis techniques to yield more valuable fine chemicals and fuels.4–9 In the former study, there are some experimental rate constants of this reaction [17-21]. In the experiment, for the $\text{C}_5\text{H}_9\text{O}$ reaction, the direct abstraction ($\text{C}_5\text{H}_8 + \text{OH}$) were found. The decomposition products of the chemically activated intermediate could be identified, and the relative products branching fractions were obtained [22]. A number of studies on thermal cyclopentoxy radical reactions are published. A few theoretical work has been done to calculate some of the reaction energies et al [23-26]. So, a thorough theoretical study of this reaction is therefore desirable to give a deep insight into the degradation reaction mechanism. The main objectives of the present article are to: (1) provide the elaborated degradation channels on the $\text{C}_5\text{H}_9\text{O}$ potential energy surface (PES), (2) investigate the possible products of the title reaction to assist in further experiment identification, and (3) give a deep insight into the degradation mechanism of $\text{C}_5\text{H}_9\text{O}$ reaction.

Computational methods

All calculations are carried out using the GAUSSIAN 03 program package [27]. All structures of the stationary points including reactants, intermediates, transition states, and products are calculated using the hybrid density functional B3LYP [28,29] method (the Becke’s three parameter hybrid functional with the

* Corresponding author. Fax: +86-471-4392124. E-mail addresses: liuhx@imnu.edu.cn, liuhongxia_101@163.com

nonlocal correlation functional of Lee–Yang–Parr) with 6-311G(d,p) basis set [30-33]. To confirm whether the transition state connects the right reactants and products, the minimum energy path (MEP) is calculated by intrinsic reaction coordinate (IRC) theory with a gradient step size of $0.05(\text{amu})^{1/2}$ bohr at the B3LYP level. To obtain more reliable energetic data, higher-level single-point energy calculations are performed at the multi-coefficient correlation method based on quadratic configuration interaction with single and double excitations (MC-QCISD) [34] by using the B3LYP/6-311G(d,p) optimized geometries. Unless otherwise specified, the B3LYP geometries and MC-QCISD single-point energies with inclusion of scaled B3LYP zero-point energies (ZPE) (simplified as MC-QCISD//B3LYP) are used in the following discussions.

II. Results And Discussion

The optimized structures of important stationary points as well as the corresponding experimental data [35-38] are depicted in Fig. 1. Note that the calculated geometries are in good agreement with experimental results with the largest deviation less than 5 at the B3LYP/6-311G(d,p) level. For our discussion easier, the energy of reactants **R** is set to be zero for reference. To clarify the reaction mechanism, the relevant pathways of PES for *c*-C₅H₉O reaction are depicted in Fig. 2.

1. Dissociation pathways

As shown in Figure 2, the ringlike reactant **R** *c*-C₅H₉O may prefer undergoing 1,3-H-shift from contiguous C atom to O atom via **TSRP₁** (19.2 kcal/mol), and form product **P₁** *c*-C₅H₈OH (-8.1 kcal/mol). A barrier of 19.2 kcal/mol is needed for conversion from **R** → **P₁**. As shown in Figure 1, the transition state **TSRP₁** has a loose CCOH four-membered ring structure, in which the distance of O-H is surprisingly long as 1.266 Å, while the C-H bond that will be broken is 1.354 Å. Alternatively, the reactant **R** also can occur the C-H bond rupture leading to **P₂** *c*-C₅H₈O + H (9.7 kcal/mol) via **TSRP₂** (17.9 kcal/mol) with the barrier height 17.9 kcal/mol. The migrating hydrogen is 1.762 Å away from the origin (C atom). In addition, the primary product **P₁** can further dissociate to give **P₃** *c*-C₅H₈ + OH (21.3 kcal/mol) via the direct C-O single bond rupture. These processes can be described as:



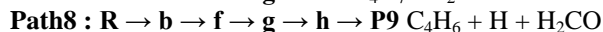
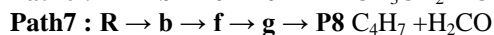
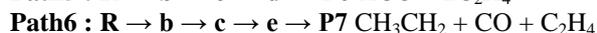
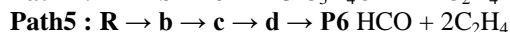
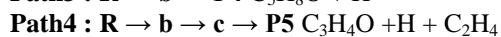
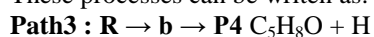
Now, we turn our attention to the other dissociation channels of reactant **R**. As shown in Figure 2, the cleavage of C-C bond of **R** may proceed to weakly bound intermediate **b** (0.4 kcal/mol) via transition state **TSRb** (9.6 kcal/mol) with the barrier of 9.6 kcal/mol. As seen in Figure 1, the **TSRb** can occur the C-C bond rupture, in which the breaking C-C bond length is 2.090 Å. The vibration mode of the imaginary frequency of **TSRb** corresponds to C-C bond stretch vibrations. Starting from the intermediate **b**, three kinds of pathways are identified: (i) the ring-closure can form the four-membered ring intermediate **f** HCO-*c*-CH₂CH₂CH₂CH₂ (34.0 kcal/mol); (ii) it occurs the H-extrusion directly to form **P₄** C₅H₈O + H (33.6 kcal/mol); (iii) we find the cleavage of the C-C bond leading to the end-C₂H₄-extrusion to form the chainlike intermediate **c** C₂H₄-CH₂CH₂CHO (21.3 kcal/mol). As shown in Figure 2, this three kinds of pathways forming **f**, **P₄**, and **c** all have the transition states, that is, **TSbf** (56.7 kcal/mol), **TSbP₄** (36.1 kcal/mol), and **TSbc** (28.7 kcal/mol), higher in energy than the intermediate **b** (0.4 kcal/mol), while lower in energy than the reactant **R**. So, pathway (i)-(iii) are all feasible pathways in thermodynamics. However, the process of pathway (ii) is completed by one-step starting from intermediate **b**, it is more simple than other two channels, we assume that pathway (ii) is favorable channel in kinetics in above three pathways.

Starting from the low-lying intermediate **c** C₂H₄-CH₂CH₂CHO (21.3 kcal/mol), there are several transform pathways, which can be generally divided into three kinds: (i) C-C rupture can form intermediate **d** HCO-CH₂CH₂ (35.2 kcal/mol), and then direct give product **P₆** HCO + CH₂CH₂ (36.0 kcal/mol); (ii) H-extrusion may be give product **P₅** C₃H₄O + H (51.2 kcal/mol); (iii) 1,3-H-shift can form ringlike intermediate **e** (14.8 kcal/mol) along with the C-C rupture to form **P₇** CH₃CH₂ + CO (16.0 kcal/mol). As seen in Figure 2, the transition states **TScd** (44.6 kcal/mol), **TScP₅** (55.3 kcal/mol), **TSce** (55.9 kcal/mol), and **TSep₇** (22.4 kcal/mol) are found in these three channels. Pathway (i) and (ii) are competitive each other, because the transition state **TScd** (44.6 kcal/mol) lie 0.6 kcal/mol lower than **TScP₅** (55.3 kcal/mol), while the product **P₆** HCO + CH₂CH₂ (36.0 kcal/mol) can discharge more energies than **P₅** C₃H₄O + H (51.2 kcal/mol). We can see that the energy of **P₇** CH₃CH₂ + CO (16.0 kcal/mol) is the lowest among the three products. The process of pathway (iii) is more complex than other two channels. So pathway (iii) is much less competitive with pathways (i) and (ii) in these three channels from intermediate **c**.

The intermediate **f** HCO-*c*-CH₂CH₂CH₂CH₂ (34.0 kcal/mol) occur 1,2-H-shift from ring to HCO to form intermediate **g** H₂CO-*c*-CHCH₂CH₂CH₂ (35.4 kcal/mol) via transition state **TSfg** (40.2 kcal/mol). Subsequently, there are two kinds of transform pathways from intermediate **g**: (i) the C-C bond can rupture along with C-C addition to form three-membered product **P₈** C₄H₇ (39.3 kcal/mol) via transition state **TSgP₈** (76.8 kcal/mol); (ii) ring- unclosure lead to intermediate **h** (31.5 kcal/mol) via **TSgh** (61.0 kcal/mol),

cooperating with H-extrusion to form **P**₉ C₄H₆ + H (54.3 kcal/mol) via **TShP**₉ (61.0 kcal/mol). Obviously, the barrier height of **TSgP**₈ higher than that of **TSgh** and **TShP**₉, channel (ii) is more favorable in kinetics. However, **P**₉ gives out more energies than **P**₈, channel (i) is feasible in thermodynamics.

These processes can be written as:



As shown in Figure 2, in terms of adiabatic potential energy, all the transition states and intermediates in **Path 1- Path 8** lie above the reactants **R**. As a result, **Path 1- Path 8** are unfavorable at normal temperature. If we want to degradate the reaction, we should try to control the pressure and the temperature.

2. Reaction mechanism and experimental implications

In the previous sections, we obtained eight important reaction channels (**Path 1-8**) that are all thermodynamically and kinetically accessible for the PES of *c*-C₅H₉O degradation reaction. There are three possible degradation reaction pathways from reactant **R**. First, **R** can directly dissociate to low-lying product **P**₁ *c*-C₅H₈OH (-8.1 kcal/mol) through the 1,3-H-shift, and then dissociate to give the secondary product **P**₃ *c*-C₅H₈ + OH (21.3 kcal/mol) via the direct C-O single bond rupture. Second, H-extrusion is occurred to form the product **P**₂ *c*-C₅H₈O + H. Third, starting from **R**, it may proceed to weakly bound intermediate **b** (0.4 kcal/mol) via C-C bond rupture transition state **TSRb** (9.6 kcal/mol) with the barrier of 9.6 kcal/mol. Isomer **b** also can dissociate to other products like **P**₄ – **P**₉ by several steps, which play an important role in organic chemistry and combustion process. As shown in Figure 2, there are three reaction pathways leading to these isomers, i.e., **R** → **P**₁ → **P**₃, **R** → **P**₂, and **R** → **b**. As discussed in section 2.1, the latter reaction pathway cannot compete with **R** → **P**₁ → **P**₃ and **R** → **P**₂. Although **R** → **b**, the conversion transition state **TSRb** lies 9.6 and 8.3 kcal/mol lower than **TSRP**₁ in **R** → **P**₁ → **P**₃ and **TSRP**₂ in **R** → **P**₂, there exit several processes to form other products. Consequently, reflected in the final product distribution, we may predict that **P**₁, **P**₂, and **P**₃ are the feasible product and the other products **P**₄ – **P**₉ can compete with **P**₁ – **P**₃.

Our result is in good agreement with kinetic study result by Karlheinz Hoyerermann et al., they proposed that *c*-C₅H₈O reaction occurs (i) 1,2 hydrogen shift to form cyclopentanone; (ii) 1,2 ring cleavage forming a noncyclic diradical, which may lead by a 1,3 hydrogen shift to 4-pentenal, or by a C-C fission to acrolein and ethene (a direct concerted formation is also possible), and by ring contraction to cyclobutylcarboxaldehyde, respectively. The observed products are *c*-C₅H₈, *c*-C₅H₈O, CH₂CH(CH₂)₂CHO, C₂H₄, C₃H₄O, 4-pentenal, OH, and H, while the major one is *c*-C₅H₈. Yet, on the basis of our present calculations, we think this reaction proceeds through a multistep process of association, isomerization, and dissociation as described by **Path 1**. Because all the isomers and transition states involved in this pathway lie above the reactants **R**, the *c*-C₅H₉O degradation reaction may be not fast. This is confirmed by Karlheinz Hoyerermann et al.' experiment.[22] In addition, several other potential products are searched. Therefore, further kinetic investigations are still required for the unobserved low-lying products CH₃CH₂, HCO, CO, and CH₃-*c*C₃H₄, and to deeply understand the mechanism of the title reaction.

III. Conclusions

The detailed potential energy surface of the degradation reaction *c*-C₅H₉O has been characterized at the B3LYP and MC-QCISD (single-point) levels. The mechanism can generally be summarized as isomerization and dissociation processes. (1) Starting from **R**, two primary products **P**₁ *c*-C₅H₈OH and **P**₂ *c*-C₅H₈O + H, one secondary product **P**₃ *c*-C₅H₈ + OH, and six lesser products **P**₄ – **P**₉ should be observed, in which **P**₁ is the more favorable product at high pressure, while at low pressure, **P**₃ may be more competitive, while **P**₂ is more competitive than **P**₁ and **P**₃. **P**₄- **P**₉ are the less feasible products. Our results agree well with the experimental observation for the title reaction. (2) Since all the involved intermediates and transition states in the unfeasible pathways **Path 1- 9** are higher than the reactants **R** in the energy, the *c*-C₅H₉O degradation reaction is expected to be not fast, which is consistent with the experimental measurement. If we want to degradate the title reaction, we should try to control the pressure and the temperature. Thus the title reaction may play an important part in atmospheric chemistry. The present theoretical studies may provide useful information on the degradation reaction mechanism for future experiments and is expected to be helpful for understanding the combustion chemistry.

Acknowledgements

The project was supported by the Higher educational Scientific research projects of Inner Mongolia (NJZY030), the Natural Science Foundation of Inner Mongolia (2012MS0218), the Talent Development Foundation of Inner Mongolia, the Inner Mongolia Normal University Research Fund Project (KYZR1119), the Natural Science Foundation of Inner Mongolia (2014BS0206), and the Scientific research project of the Inner Mongolia colleges and Universities (NJZY030). The authors are grateful to the referee for his valuable comments on improving the manuscript.

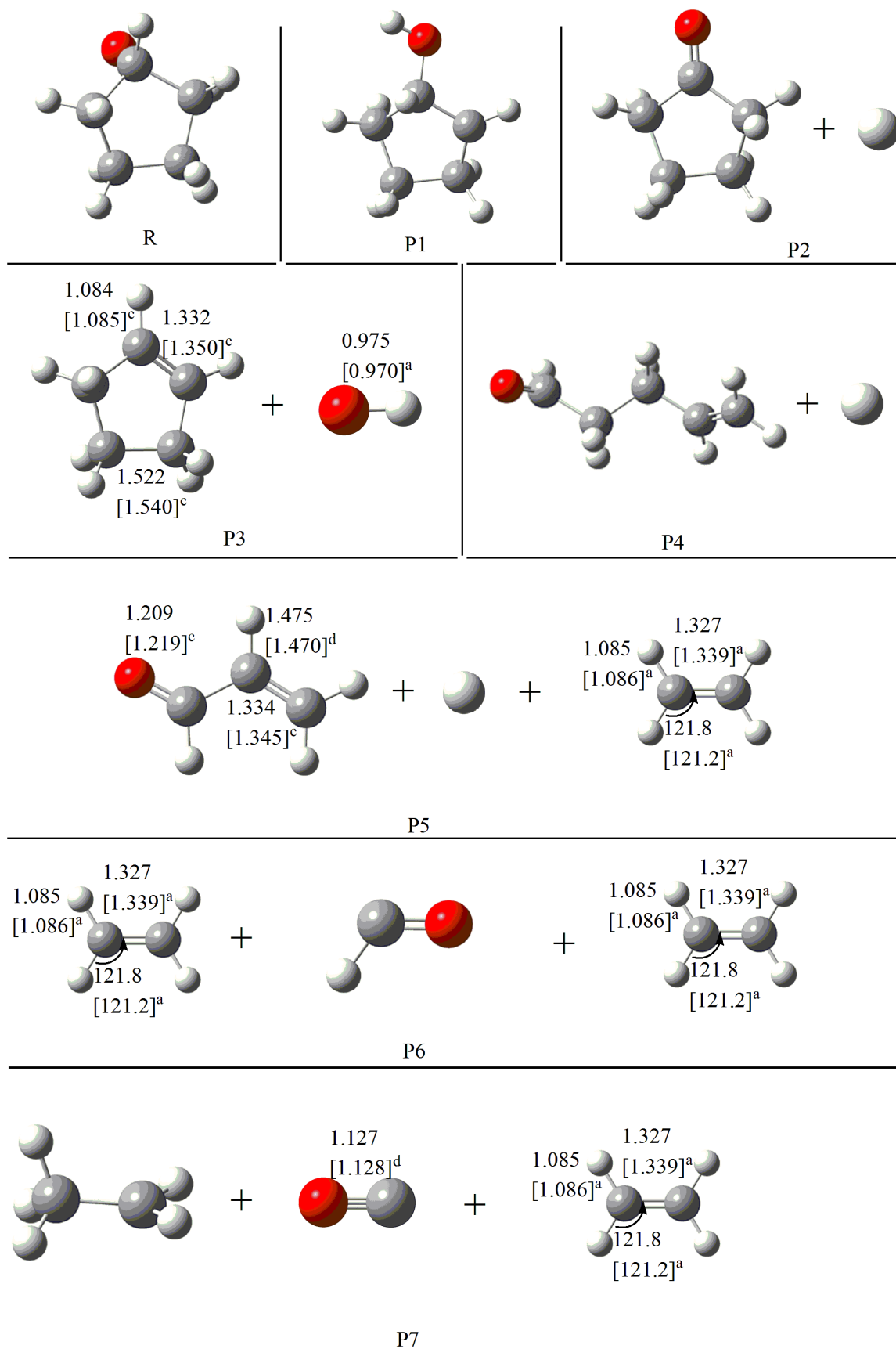
References

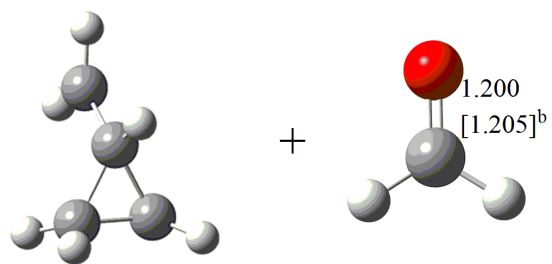
- [1]. Tsang W, Hampson R.F (1986) J. Phys. Chem. Ref Data. 15:1087-1279
- [2]. Warnatz J, In:Gardiner WC (1984) Jr (ed)Combustion Chemistry. Springer, New York
- [3]. Singh H.B, Zimmerman P.R Atmospheric Distribution and Sources of Nonmethane Hydrocarbons, In Gaseous Pollutants: Characterization and Cycling; Nriagu, J. O (1992) Ed.; John Wiley: New York, 177-235
- [4]. Harley R.A, Cass GR (1995) Atmos. Environ. 29:905
- [5]. Takagi H, Washida N, Bandow H, Akimoto H, Okuda M (1981) J. Phys. Chem. 85:2701-2705
- [6]. Atkinson R, Aschmann S.M, Carter W.P.L, Winer A.M, Pitts J.N.Jr (1984) Int. J. Chem. Kinet. 16: 1085-1101
- [7]. Wu D, Bayes K.D (1986) Int. J. Chem. Kinet. 18: 547-554
- [8]. Rowley D.M, Lightfoot P.D, Lesclaux R, Wallington T.J (1991) J. Chem. Soc., Faraday Trans. 87: 3221-3226
- [9]. Rowley D.M, Lightfoot P.D, Lesclaux R, Wallington T.J (1992) J. Chem. Soc., Faraday Trans. 88: 1369-1376
- [10]. Rowley D. M, Lesclaux R, Lightfoot P. D, Nozie`re B, Wallington T. J, Hurley M. D (1992) J. Phys. Chem. 96: 4889-4894
- [11]. Atkinson R, Aschmann S. M, Arey J, Shorees B. (1992) J Geophys. Res. 97: 6065
- [12]. Crawford M. A, Szenté J. J, Maricq M. M, Francisco J. S (1997) J. Phys. Chem. A. 101: 5337-5343
- [13]. Aschmann S. M, Chew A. A, Arey J, Atkinson R (1997) J. Phys. Chem. A. 101: 8042-8048
- [14]. Platz J, Sehested J, Nielsen O. J, Wallington T. J (1999) J. Phys. Chem. A. 103: 2688-2695
- [15]. (a) Kochi J. K (1962) J. Am. Chem. Soc. 84:1193-1197 (b) Kochi J. K Free Radicals; Kochi J. K (1973) Ed Wiley-Interscience: New York, 2:665 (c) Gray P, Williams A (1959) Chem. Rev. 59:239
- [17]. Hoyermann K, Olzmann M, Zeuch T (2002) Proc. Combust. Inst. 29:1247-1255
- [18]. Hoyermann K, Nacke F (1996) Proc. Combust. Inst. 26:505-512
- [19]. Heinemann-Fiedler P, Hoyermann K, Rohde G (1990) Ber. Bunsen-Ges. Phys. Chem. 94:1400-1404
- [20]. Hack W, Hold M, Hoyermann K, Wehmeyer J, Zeuch T (2005) Phys. Chem. Chem. Phys. 7:1977-1984
- [21]. Rohde G (1991) Ph.D. Thesis, Go'ttingen
- [22]. Karlheinz H, Nothdurft J, Olzmann M, Wehmeyer J, and Zeuch T (2006) J. Phys. Chem. A 110:3165-3173
- [23]. Beckwith A. L. J, Hay B. P (1989) J. Am. Chem. Soc. 111:230-234
- [24]. Wilsey S, Dowd P, Houk K. N (1999) J. Org. Chem. 64:8801
- [25]. Orlando J. J, Iraci L. T, Tyndall G. S (2000) J. Phys. Chem. A. 104:5072-5079
- [26]. Alconcel L. S, Continetti R. E (2002) Chem. Phys. Lett. 366:642-649
- [27]. Frisch M J, Trucks G W, Schlegel H B, Scuseria G E, Robb M A, Cheeseman J R, Montgomery J A Jr, Vreven T, Kudin K N, Burant J C, Millam J M, Iyengar S S, Tomasi J, Barone V, Mennucci B, Cossi M, Scalmani G, Rega N, Petersson G A, Nakatsuji H, Hada M, Ehara M, Toyota K, Fukuda R, Hasegawa J, Ishida M, Nakajima T, Honda Y, Kitao O, Nakai H, Klene M, Li X, Knox J E, Hratchian H P, Cross J B, Adamo C, Jaramillo J, Gomperts R, Stratmann R E, Yazyev O, Austin A J, Cammi R, Pomelli C, Ochterski J W, Ayala P Y, Morokuma K, Voth G A, Salvador P, Dannenberg J J, Zakrzewski V G, Dapprich S, Daniels A D, Strain M C, Farkas O, Malick D K, Rabuck A D, Raghavachari K, Foresman J B, Ortiz J V, Cui Q, Baboul A G, Clifford S, Cioslowski J, Stefanov B B, Liu G, Liashenko A, Piskorz P, Komaromi I, Martin R L, Fox D J, Keith T, Al-Laham M A, Peng C Y, Nanayakkara A, Challacombe M, Gill P M W, Johnson B, Chen W, Wong M W, Gonzalez C, Pople J A (2003) Gaussian 03, Revision B.04. Gaussian, Pittsburgh PA
- [28]. Becke A.D (1992) J. Chem. Phys. 97: 9173-9177
- [29]. Lee C, Yang W, Parr R.G (1988) Phys. Rev. 37:785-
- [30]. Becke A.D. (1993) J. Chem. Phys. 98:5648-5652
- [31]. McLean A.D, Chandler G.S. (1980) J. Chem. Phys. 72:5639-5648
- [32]. Krishnan R, Binkley J.S, Seeger R, Pople J.A. (1980) J. Chem. Phys. 72:650-654
- [33]. Frisch M.J, Pople J.A, Binkley J.S (1984) J. Chem. Phys. 80:3265-3269
- [34]. Fast P L, Truhlar D G (2000) J Phys Chem A 104:6111-6116
- [35]. Herzberg G (1966) Electronic spectra and electronic structure of polyatomic molecules, Van Nostrand, New York
- [36]. Gurvich L. V, Veys I. V, Alcock C. B (1989) Thermodynamic Properties of Individual Substances, Fourth Edition, Hemisphere Pub. Co., New York
- [37]. Hellwege K H and Hellwege A M (1976) (ed.). Landolt-Bornstein: Group II: Atomic and Molecular Physics Volume 7: Structure Data of Free Polyatomic Molecules. Springer-Verlag, Berlin
- [38]. Huber K.P, Herzberg G (1979) Molecular Spectra and Molecular Structure. IV. Constants of Diatomic Molecules., Van Nostrand Reinhold Co.

Figure Caption

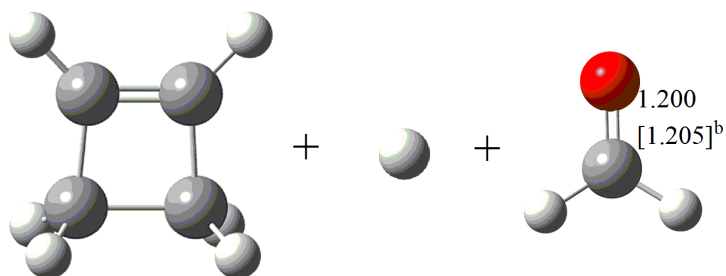
Figure 1: The B3LYP/6-311G(d,p) optimized geometries of reactants, products, complexes, and transition states for c-C₅H₉O reaction. Bond distances are in angstroms and angles are in degrees. The values obtained with the B3LYP/6-311G(d,p) method and the experimental values are also given in square brackets. (^aValues from ref.³⁵, ^bValues from ref.³⁶, ^cValues from ref.³⁷, ^dValues from ref.³⁸)

Figure 2: Schematic potential energy surface of the reaction channels for the c-C₅H₉O reaction at the MC-QCISD//B3LYP/6-311G(d,p) + ZPE level. E_{rel} are the relative energies (kcal/mol).

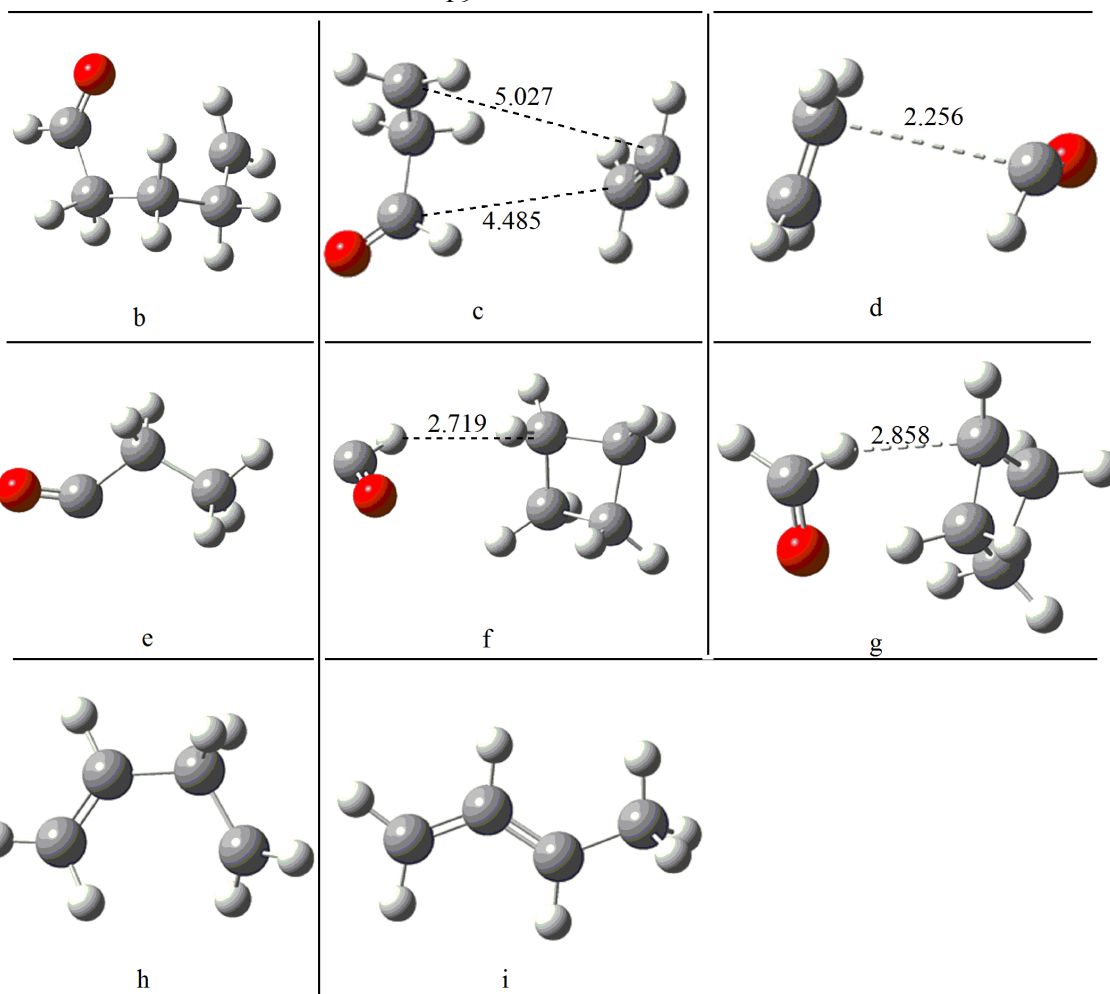


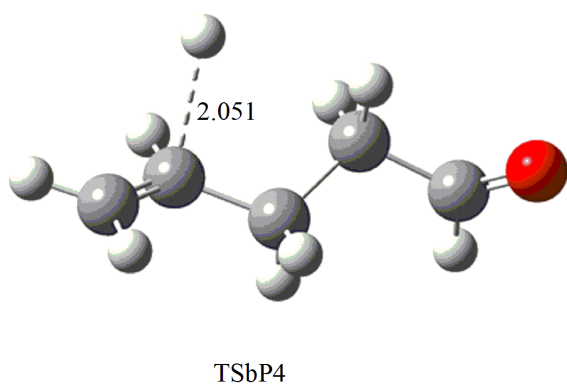
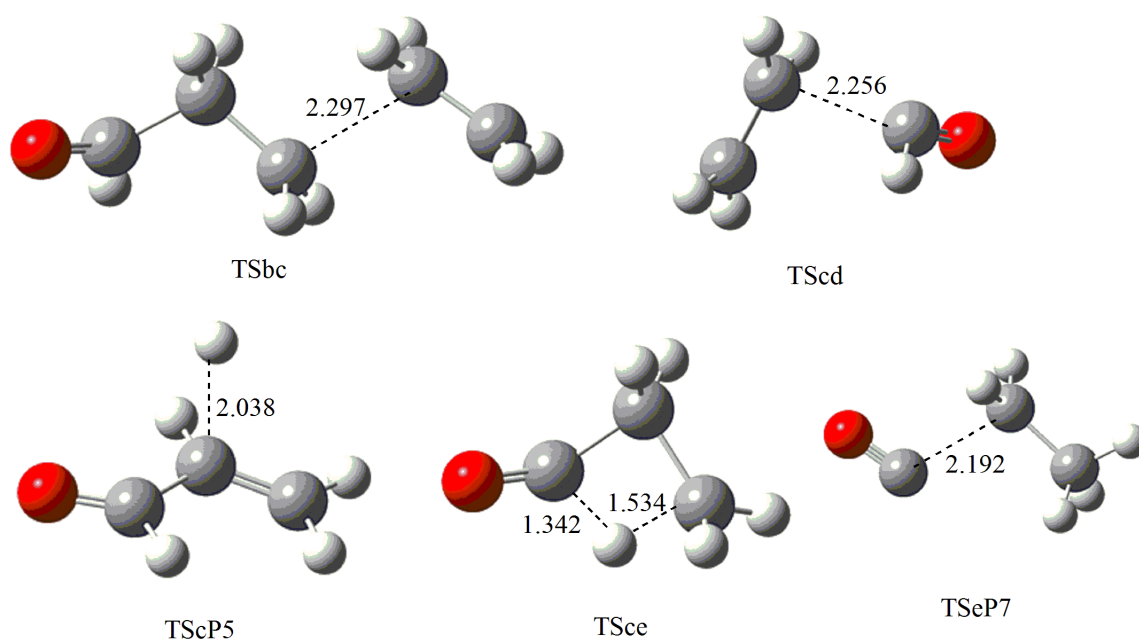
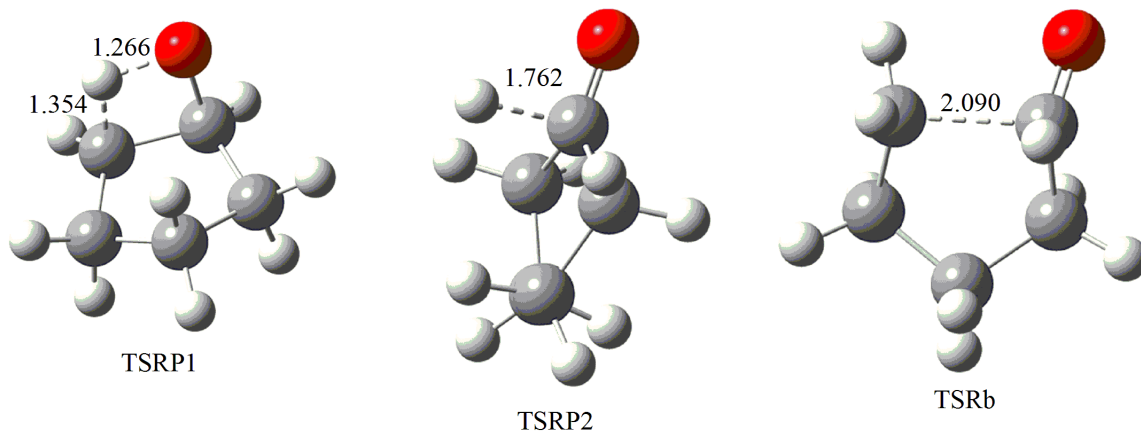


P8



P9





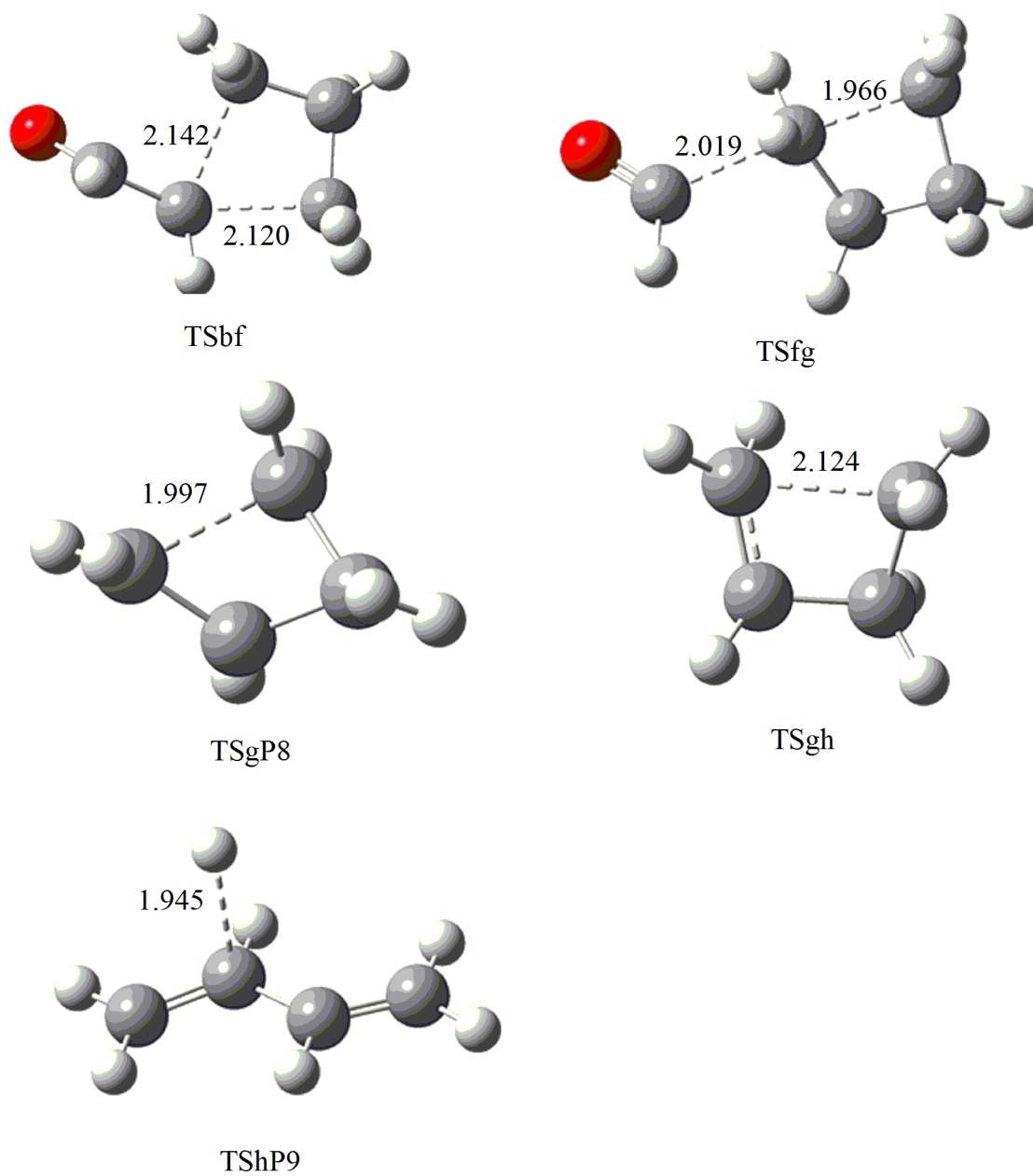


Figure 1

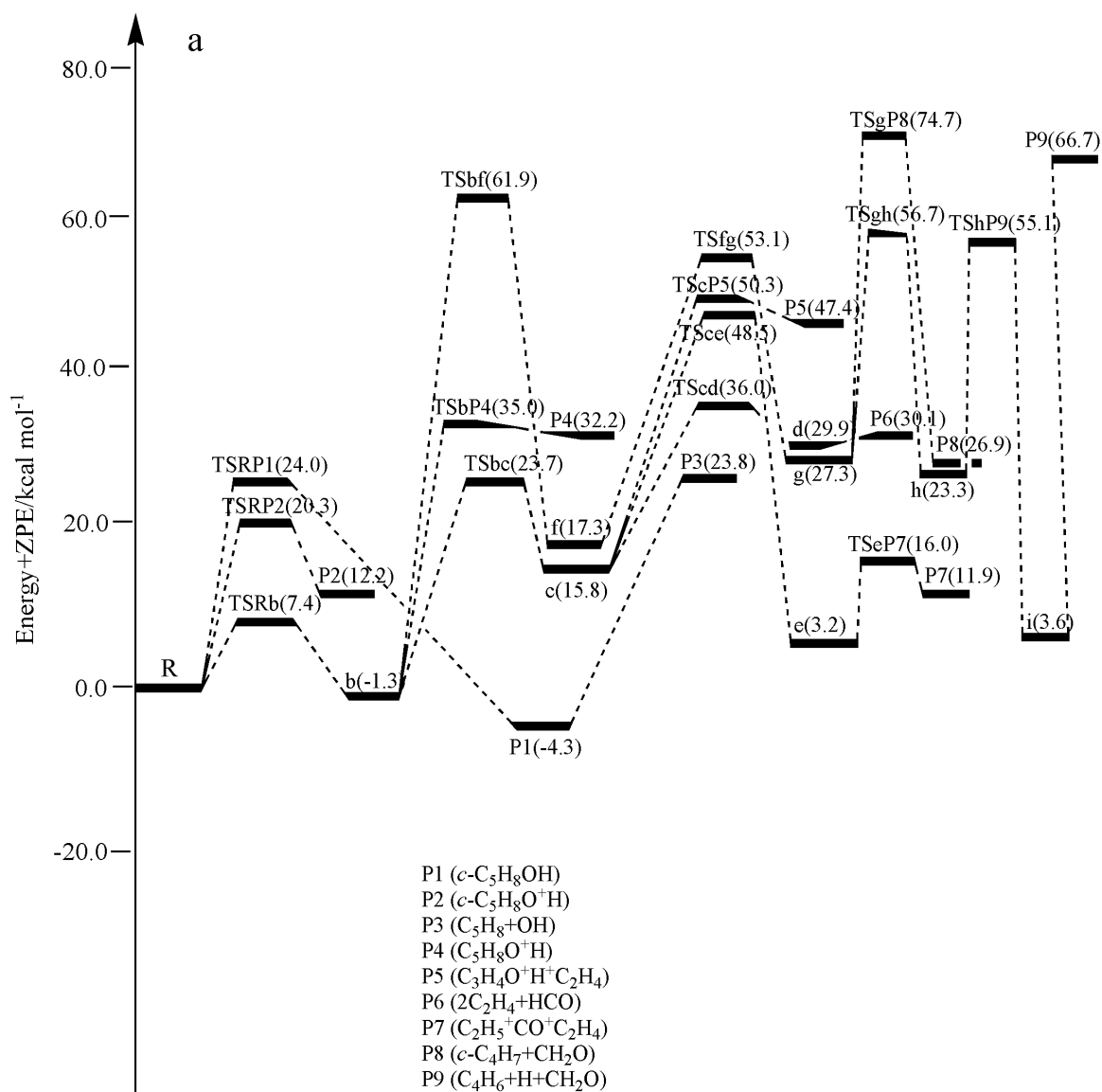


Figure 2

Hongxia Liu" Study on the Degradation Mechanism of the Cyclopentaneoxygen free radicals: *c*-C₅H₉ Radical with O(3p) radical." IOSR Journal of Applied Chemistry (IOSR-JAC) 12.6 (2019): 23-31.